Romanian Reports in Physics, Vol. 63, Supplement, P. 1236–1253, 2011

Dedicated to Professor Marin Ivaşcu's 80th Anniversary

LOW-HEAT SOLID-STATE LASERS

V. LUPEI[1,2]

[1]Romanian Academy, Section Physics, Bucharest, Romania
[2]National Institute of Laser, Plasma and Radiation Physics, Magurele-Bucharest, Romania
E-mail: lupei_voicu@yahoo.com

Received June 30, 2011

Abstract. The paper discusses the processes that determine the parasitic heat generation and its distribution in the solid-state laser materials. It is inferred that the balance between the laser emission and heat generation is determined by the characteristics of the pumping system and by the partial efficiencies of the various steps of the flow of excitation between the energy levels of the laser material and the design of laser resonator contributes to the spatial distribution of thermal field. Solutions for improvement of this balance and for scaling to high power are discussed

Key words: solid-state lasers, de-excitation processes, laser emission, heat generation.

1. INTRODUCTION

The solid-state lasers are the solution of choice for many applications of lasers in medicine, processing of materials, monitoring of environment, nuclear physics and energy, defense and security and so on. These lasers could provide coherent radiation at various wavelengths from UV to MID-IR by fundamental emission or nonlinear conversion of this emission, whereas the temporal regime extends from continuous-wave emission to very short (femtosecond) pulses. The power range of the individual, coupled or amplified solid-state laser beams extends now to hundred kW in continuous-wave and in free-generation pulsed regime and to PW peak power in short-pulse emission whereas the pulse energy can reach tens of kilojoules per beam. Despite of these impressive performances, the extension of applications requires further development along directions such as efficiency, wavelength range, temporal regime, beam quality, power or energy scaling [1].

The active materials for the solid-state lasers are transparent solids activated with ions from the transition groups, especially trivalent rare-earth ions RE^{3+}, such as Nd^{3+}, Yb^{3+}, Er^{3+} and so on, whose ground electronic configuration contains incomplete 4f electronic shell. The optical processes (absorption or emission of radiation) take place by transitions between the Stark components of the energy

manifolds inside of the ground electronic configuration. Since the quantum states of the doping ions (energy levels, transition probabilities) are determined by the interaction with the particular crystal field in each laser material, the characteristics of the optical transitions (wavelength, cross-section) will be different for a given RE^{3+} ion in various laser materials and this situation generates a very large basis of selection. The complex energy level structure of most RE^{3+} ions could accommodate one or several four-level or (quasi) three-level lasers schemes.

The performances of the solid-state lasers are determined by the capability of the laser material to absorb the pump radiation and by the utilization of the absorbed power for laser emission. The laser emission schemes assume an energy quantum defect between the pump and laser radiation. The absorption of the pump radiation is assumed on transitions with suitable cross-sections between the ground energy level $E_g = 0$ to the pump absorbing energy level E_p and can be further controlled by proper choice of the doping concentration and of the path of pump radiation inside the laser material. The excitation fed into the pump level decays by fast non-radiative processes to the emitting level E_{em} from which optical emission to the terminal level E_t take place and the excitation of this level relaxes by very fast non-radiative processes to the ground level. Thus, the whole energy corresponding to the absolute quantum defect $\Delta E_{qd} = (E_p - E_g) - (E_{em} - E_t)$ is transformed by the electron-phonon relaxation into heat.

In a real laser not all the laser ions excited to the emitting level E_{em} participate in the lasing process. The excited ions that form the population of this level below the laser threshold as well as those placed in the pumped volume outside the laser mode volume de-excite by luminescence and by non-radiative processes such as energy transfer inside the system of doping ions or to accidental impurities and electron-phonon interaction, the proportion between the radiative and non-radiative processes being expressed by the emission quantum efficiency. In most cases, the final states of the donor and acceptor ions involved in the energy transfer de-excite further by electron-phonon interaction and thus all the excitation lost by non-radiative processes transforms into heat. Another difference between these classes of excited ions is determined by the characteristics of the radiative processes: whereas the laser emission takes place at a fixed wavelength, and thus the quantum defect is well defined, the luminescence can take on various transitions, with specific wavelengths, to several lower energy levels and an average emission wavelength must be defined, that determines an effective quantum defect.

According to this discussion, the heat generation in the laser materials has two components, the quantum defect and the non-radiative de-excitation of the emitting level for the excited ions that do not participate to lasing: whereas the former effect is determined by the energy levels of the doping ions and by the

emission and pump wavelengths, the later are influenced by factors as the doping concentration and electron-phonon de-excitation of the emitting level. It is then obvious that the heat generation by these two classes of excited would be different and their relative contribution to the heat generation is determined by the superposition of the pump and laser volume and by the operating point above threshold; moreover, these factors determine a specific spatial distribution of heat generation.

The heat generated by the non-radiative processes raises the temperature of the laser material and thus the distribution of heat generation determines a distribution of local temperatures. *i.e.* a specific thermal field configuration. The thermal field inside the laser material induces spatially-distributed thermo-mechanical and thermo-optic effects that can damage the laser material or/and distort the wave-front of the laser emission and determines the need for forced external cooling. Limitation of these effects impose dissipation of heat and this is usually achieved by forced external cooling. The cooling could modify severely the configuration of the thermal field in the laser material, resulting in thermo-optical effects such as thermal lensing that can destroy the condition of amplification of the laser resonator. Since the heat generation increases with the absorbed pump power, these thermo-optical effects will further limit the power scaling. Thus, despite of the sustained effort for mitigation of the thermal effects and for engineering of cooling [2], reduction of heat generation remains major point of concern in power scaling.

This paper discusses the heat generation, based on the analysis of the relevant steps of the flow of excitation inside the electronic structure of the laser active ions. It is thus shown that the global efficiencies of the de-excitation processes (laser, luminescence, heat generation) can be expressed by the individual efficiencies of each of these steps in the flow of excitation and, in turn, these individual efficiencies are accurately determined by the characteristics of the laser material, pumping system and laser resonator. Based on these dependences, directions for controlling the heat generation in solid-state lasers are envisaged.

2. THE STEPS IN THE FLOW OF EXCITATION INSIDE THE PUMPED LASER MATERIAL

Figure 1 shows schematically the steps in the flow of excitation inside the energy level structure of a four-level laser material. The four laser levels (E_g, E_t, E_{em} and E_p, in ascending order) is embedded in a more complex energy level scheme (the Stark components of the various energy manifolds) of a doping laser ion and several of the additional levels could influence the de-excitation processes.

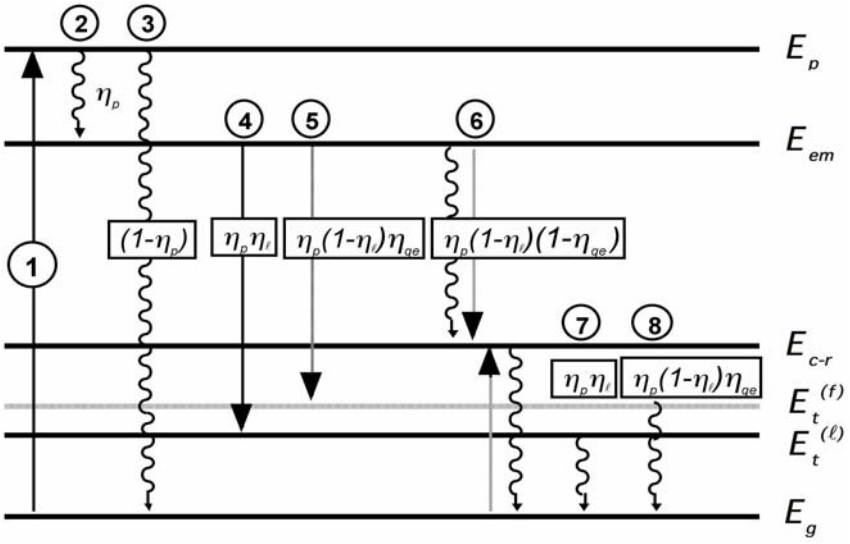

Fig. 1 – The flow of excitation in the four-level laser material.

The situation presented in Fig. 1 approaches the complex case of the Nd^{3+}-doped laser materials pumped resonantly with diode lasers (process **1**): the level E_p could be the manifold $^4F_{5/2}$ that can be pumped by the 808 nm diode lasers, the emitting level E_{em} is the unique metastable level $^4F_{3/2}$, the terminal level for the laser emission $E_t^{(l)}$ can be either the manifold $^4I_{13/2}$ (1.32 μm laser), $^4I_{11/2}$ (for 1.06 μm laser), or $^4I_{9/2}$ (0.94 μm laser) and the ground state is $^4I_{9/2}$. The ions that do not lase can de-excite by luminescence on the various transitions to Stark levels of the lower manifolds $^4I_{9/2,11/2,13/2,15/2}$; these luminescence processes can be characterized by an average wavelength, that defines an effective terminal level for the luminescence, $E_t^{(f)}$. The energy level E_{c-r} (the energy manifold $^4I_{15/2}$ in case of Nd^{3+}) enables the non-radiative de-excitation of $^4F_{3/2}$ by cross-relaxation energy transfer of the emitting level by interaction with an unexcited Nd^{3+} ion. The absorbed pump radiation is thus consumed in a complex chain of radiative and non-radiative de-excitation processes, specific for each level from the laser scheme.

2.1. THE EMISSION QUANTUM DEFECT

The radiative processes are characterized by specific absolute quantum defects,

$$\Delta E_{qd}^{(l)} = (E_p - E_g) - (E_{em} - E_t^{(l)}), \tag{1}$$

$$\Delta E_{qd}^{(f)} = (E_p - E_g) - (E_{em} - E_t^{(f)}) . \quad (2)$$

The quantum defect can be also expressed relative to the pump energy quantum,

$$QD^{(l)} = \frac{\Delta E_{qd}^{(l)}}{E_p} = 1 - \frac{\lambda_p}{\lambda_l} = 1 - \eta_{qd}^{(l)} , \quad (3)$$

$$QD^{(f)} = \frac{\Delta E_{qd}^{(f)}}{E_p} = 1 - \frac{\lambda_p}{\overline{\lambda}} = 1 - \eta_{qd}^{(f)} . \quad (4)$$

In these equations $\eta_{qd}^{(em)} = \lambda_p / \lambda_{em}$ represent the quantum defect (Stokes) ratio. The average luminescence emission wavelength can be calculated by using the branching ratios and the wavelengths of the various luminescence emission lines from the emitting level, $\overline{\lambda} = \sum \beta_i \lambda_i$: in case of Nd:YAG $\overline{\lambda} = 1038$ nm.

The quantum defect is composed of two parts, the upper (superior) part $\Delta E_{qd}^{(up,em)} = E_p - E_{em}$ and the lower (inferior) part $\Delta E_{qd}^{(low,em)} = E_t^{(em)} - E_g$; for the emission processes represented in Fig. 1, the upper quantum defect is the same for the laser and luminescence emission, whereas the lower quantum defect is different. According to this scheme, the upper quantum defect is introduced only by reason of high absorption efficiency, whereas the lower quantum defect is a characteristic of the emission process.

2.2. THE DE-EXCITATION OF THE PUMP LEVEL

By the definition of the four level scheme, a very fast de-excitation from the strongly absorbing pump level E_p to the emitting level E_{em}, should take place. (process **2**). However, several works [3, 4] claim that a very efficient transfer of excitation from E_p to accidental nearby anionic impurities with high vibrational quanta could take place and this can divert part of excitation fed in the level E_p from reaching the emitting level (process **3**). The excitation transferred to these accidental impurities would relax rapidly to the ground state and thus the crystal sites occupied by doping laser ions with nearby such anionic impurities were called "dead sites" This model was introduced as possible explanation for the reduced emission efficiency in the Nd:YAG crystals, but the presence of such sites was never proved by any clear experimental evidence [5, 6]. In order to account for such possible parasitic de-excitation, the transfer of excitation from the pump level to the emitting level is expressed by the pump level efficiency η_p that represent the fraction of excited ions in the level E_p which reach the level E_{em}.

2.3. DE-EXCITATION OF THE EMITTING LEVEL

The proportion of excited ions that give laser emission is expressed by the laser emission efficiency $\eta_l = \eta_v(1 - f_{th})$, where η_v is the efficiency of superposition of the laser mode and pumped volumes ($\eta_v = 1$ when the laser mode volume is larger than the pumped volume and < 1 in the opposite situation) and f_{th} is the fraction of excited ions corresponding to the laser threshold, and it can be related to the operating point $f_{th} \cong (P / P_{th})^{-1}$.

2.3.1. De-excitation by laser emission

Once the laser threshold is reached, the stimulated emission becomes the dominant de-excitation process. The de-excitation by laser emission in various temporal regimes is governed in specific manner by the properties of the laser material, pumping system and laser design. Thus, in case of four-level laser free generation under continuous-wave pumping, the output power above the laser threshold $P_{th}^{(in)}$ can be related to the input power $P^{(in)}$ by the slope efficiency $\eta_{sl}^{(in)}$, *i.e.*

$$P_{out} = \eta_{sl}^{(in)}(P^{(in)} - P_{th}^{(in)}),$$

where

$$P_{th}^{(in)} = \frac{1}{2}\frac{Ah\nu_l}{\eta_a \eta_p \eta_{qd}^{(l)} \eta_v \tau_{eff} \sigma_{eff}}(T + L), \tag{5}$$

$$\eta_{sl}^{(in)} = \eta_a \eta_p \eta_{qd}^{(l)} \eta_v \frac{T}{T + L}. \tag{6}$$

In these equations T represents the transmission of the exit mirror of the laser, L are the residual optical losses at the laser wavelength, A is the area of the laser beam, τ_{eff} is the effective lifetime of the luminescence emission and σ_{eff} is the effective emission cross-section of the specific laser transition.

An optical-optical efficiency can be defined such as $P_{out} = \eta_{o-o}^{(in)} P_{in}$:

$$\eta_{o-o}^{(in)} = \eta_{sl}^{(in)}\left(1 - \frac{P_{th}^{(in)}}{P^{(in)}}\right) = \eta_a \eta_p \eta_{qd}^{(l)} \eta_v \left(1 - \frac{P_{th}^{(in)}}{P^{(in)}}\right)\frac{T}{T + L} = \eta_a \eta_p \eta_{qd}^{(l)} \eta_l \frac{T}{T + L}. \tag{7}$$

These laser parameters can be also expressed in absorbed power by using the relation $P^{(a)} = \eta_a P^{(in)}$. The fraction of the absorbed excitation found in the laser emission in absence of any losses *L* (process **4** in Fig. 1) equals $\eta_p \eta_l$.

2.3.2. De-excitation in absence of laser emission

In absence of laser emission the emitting level can de-excite by luminescence or non-radiative processes (electron-phonon interaction, energy transfer), their proportion being defined by the emission quantum efficiency η_{qe} and thus in presence of laser emission the fraction of ions that de-excite by luminescence (process **5**) is $\eta_p(1-\eta_l)\eta_{qe}$, whereas the fraction of those de-excited by the non-radiative processes **6** is $\eta_p(1-\eta_l)(1-\eta_{qe})$.

Since the non-radiative processes reduce the amount of excited ions able to give luminescence, the emission quantum efficiency can be measured by comparing the number of emitted photons with that of absorbed photons. However, such measurements imply calibration techniques that introduce a high degree of inaccuracy. On other hand, the non-radiative processes accelerate the emission decay $I(t)$ under short pulse excitation and can modify its shape and thus a more convenient method would be to calculate the emission quantum efficiency by using these effects. In presence of pure radiative de-excitation the emission decay is exponential and can be characterized by a radiative lifetime τ_{rad} according to $I_{rad}(t) = I_{rad}(0)\exp(-t/\tau_{rad})$ and $\int_0^\infty (I_{rad}(t)/I_{rad}(0))\,\mathrm{d}t = \tau_{rad}$. The non-radiative de-excitation by electron-phonon interaction influences in an identical manner all the excited laser ions and can be characterized by a temperature-dependent de-excitation rate W_{nr}: the decay remains exponential and is characterized by a luminescence lifetime τ_f, such that $(\tau_f)^{-1} = (\tau_{rad})^{-1} + W_{nr}$. The emission quantum efficiency in this case can be calculated simply by the ratio $\eta_{qe} = \tau_f/\tau_{rad}$; however, whereas the luminescence lifetime τ_f can be measured directly from experiment, the radiative lifetime must be calculated from first principles [7, 8]. Since this calculation can introduce large errors it the radiative lifetime is assimilated with the luminescence lifetime measured at low temperature and doping concentrations, where the non-radiative processes are very weak.

The effect of energy transfer is more complex: by multipole electrostatic or superexchange interaction between an excited ion and an unexcited ion the first (the donor D) can transfer part or all its excitation to the second (the acceptor A) ion. By this process the excitation of the donor is lowered (down-conversion) whereas that of the acceptor is enhanced by a nearly resonant amount [9, 10]. The energy transfer assumes the existence of energy levels that could serve as final energy states for the donor and acceptor ions: in case of Nd^{3+} ions such intermediate state for the down-conversion could be the level $^4I_{13/2}$ that is placed in

energy at around half of the energy of the emitting level $^4F_{3/2}$ and thus it could become the final state for both the donor and acceptor ions, according to the cross-relaxation scheme ($^4F_{3/2}$, $^\$I_{9/2}$) → ($^4I_{15/2}$, $^4I_{15/2}$). The energy transfer is thus a noteworthy case of transitions between the energy levels of a quantum system under the action of static electric multipole or exchange interactions. At strong pump intensities that determine high population of the excited level, the energy transfer can take place between excited ions too, and in such cases the acceptor ion is promoted to an energy state higher than the initial state (upconversion). Moreover, at high donor concentrations, the migration of excitation on the donor ions prior to the transfer to acceptor can take place (migration-assisted transfer). Both these types of energy transfer (down- and upconversion) inside the system of doping ions reduce the population of the excited level and thus they can modify the emission decay and quantum efficiency (self-quenching of emission).

The direct donor-acceptor energy transfer rate depends on the distance between the donor and acceptor ion and on the type of ion-ion interaction and on the microparameters of transfer C_{DA}, determined by the spectroscopic properties of the donor and acceptor ion, particularly on the superposition of the donor emission with the acceptor absorption on the transitions involved in transfer. Because the acceptor ions can be placed at different distances from donor in a crystalline lattice, the global effect of the transfer on the decay of all the donor ions from material would be a non-exponential decay $I(t) = I(0)\exp(-t/\tau_D)\exp\left[-P(t)\right]$, where $\exp\left[-P(t)\right]$ is the acceptor-ensemble averaged probability that the donor is not de-excited at the time t by energy transfer. The calculation of the energy transfer function $P(t)$ depends on the model of distribution of the doping ions in the crystalline lattice (continuous or discrete, uniform or correlated) used for averaging. Generally, the energy transfer function $P(t)$ is not linear function on time and this determines the departure of the decay from exponential [9-12]. The analysis of the emission decay function on temperature, excitation intensity and doping concentrations enables evaluation of the characteristic energy transfer parameters and of the type of distribution. Similar to the lifetime of radiative de-excitation, an effective lifetime can be calculated, $\tau_{eff} = \int\left\{\exp(-t/\tau_f)\exp\left[-P(t)\right]\right\}\mathrm{d}t$ and then the emission quantum efficiency is given by $\eta_{qe} = \tau_{eff}/\tau_{rad}$. Such detailed analysis was performed for several laser materials, particularly Nd-doped yttrium aluminum garnet (YAG) [5, 6, 13-15], and the calculated Nd concentration dependence of η_{qe} at low excitation intensity, when only down-conversion processes are active, is shown in Fig. 2 and is confirmed by the various experimental measurements, assuming $\eta_p = 1$.

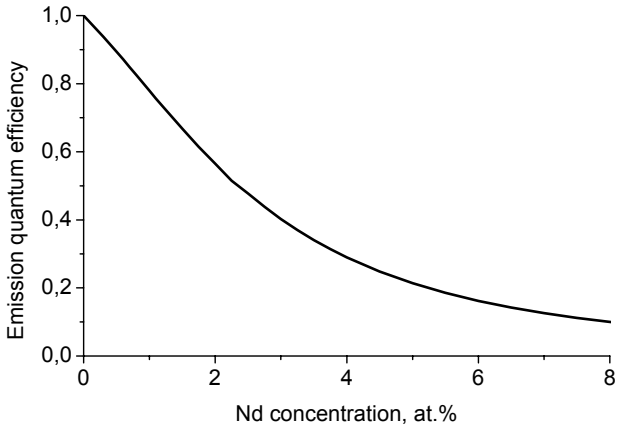

Fig. 2 – Calculated emission quantum efficiency for Nd:YAG.

2.4. DE-EXCITATION OF THE TERMINAL LEVELS OF THE RADIATIVE AND ENERGY TRANSFER PROCESSES

By definition, the terminal level of the laser emission $E_t^{(l)}$ de-excites to the ground level by very fast electron-phonon relaxation processes. Moreover, in most cases between the terminal levels of the luminescence (expressed by the effective level $E_t^{(f)}$ or of energy transfer cross-relaxation (E_{c-r}) and the ground level E_g there is a quite dense ladder of energy levels and the excitation of these terminal levels is consumed in successive very fast low-order electron-phonon processes.

3. MANIFESTATION OF THE DE-EXCITATION PROCESSES

The de-excitation processes in the flow of excitation inside the pumped laser material placed in the laser resonator manifest as radiative processes (laser and luminescence) or as heat generation by non-radiative processes (multiphonon relaxation or energy transfer followed by multiphonon relaxation). Each of these processes can be characterized by the energy ΔE dissipated in the process and by its fraction $\eta = \Delta E / E_p$ from the excitation energy and these characteristics can be expressed with the partial efficiencies defined above.

3.1. LASER EMISSION

The energy dissipated in laser emission (process **4**) and the corresponding fractional coefficient are

$$\Delta E^{(l)} = \eta_l \eta_p (E_{em} - E_t^{(l)}), \tag{8}$$

$$\eta^{(l)} = \frac{\Delta E^{(l)}}{E_p} = \frac{\eta_l \eta_p (E_{em} - E_t^{(l)})}{E_p} = \eta_l \eta_p \eta_{qd}^{(l)}. \tag{9}$$

$\eta^{(l)}$ is identical to optical-optical efficiency in absorbed power for $L = 0$.

3.2. LUMINESCENCE

The energy dissipated in the luminescence emission (process **5**) and the corresponding fractional emission coefficient are

$$\Delta E^{(f)} = (1 - \eta_l)\eta_p \eta_{qe} (E_{em} - E_t^{(f)}), \tag{10}$$

$$\eta^{(f)} = \frac{\Delta E^{(f)}}{E_p} = \frac{(1 - \eta_l)\eta_p \eta_{qe} (E_{em} - E_t^{(f)})}{E_p} = (1 - \eta_l)\eta_p \eta_{qe} \eta_{qd}^{(f)}. \tag{11}$$

3.3. HEAT GENERATION

The total energy dissipated in the non-radiative processes **2**, **3**, **6**, **7**, and **8** and the corresponding fractional coefficient are

$$\Delta E^{(nr)} = E_p - \eta_p \eta_l (E_{em} - E_t^{(l)}) - \eta_p (1 - \eta_l)\eta_{qe} (E_{em} - E_t^{(f)}), \tag{12}$$

$$\eta^{(nr)} \equiv \eta_h = \frac{\Delta E^{(nr)}}{E_p} = 1 - \eta_l \eta_p \eta_{qd}^{(l)} - (1 - \eta_l)\eta_p \eta_{qe} \eta_{qd}^{(f)}; \tag{13}$$

obviously, $\eta^{(l)} + \eta^{(f)} + \eta^{(nr)} = 1$.

The fractional heat load parameter η_h reflects the contribution to heat generation of the ions that de-excite by laser emission and of those that do not participate to lasing [4]. In absence of laser emission ($\eta_l = 0$),

$$\eta_h^{(f)} = 1 - \eta_p \eta_{qe} \eta_{qd}^{(f)}, \tag{14}$$

whereas for the excited ions that participate to the laser emission

$$\eta_h^{(l)} = 1 - \eta_p \eta_{qd}^{(l)}. \tag{15}$$

For the usual case ($\eta_p = 1$), $\eta_h^{(l)}$ equals the relative quantum defect $\mathrm{QD}^{(l)}$ given by Eq. (3) and is thus dependent only on the wavelengths of the pump and laser radiation. However, the heat generated by the ions that do not participate to the

laser emission depends also on the emission quantum efficiency, and thus on the doping concentration; moreover, in case of high excitation intensities that can onset upconversion processes, the heat generation by the ions that do not participate to the laser emission will depend additionally on the pump intensity.

According to the equations (14) and (15), when $\eta_{qd}^{(l)} = \eta_{qe}\eta_{qd}^{(f)}$, the equality $\eta_h^{(l)} = \eta_h^{(f)}$ holds. However, when $\eta_{qd}^{(l)} > \eta_{qe}\eta_{qd}^{(f)}$ the heat generated by the excited ions participating to the laser process is smaller than for the non-lasing ions, $\eta_h^{(l)} < \eta_h^{(f)}$; obviously, when $\eta_{qd}^{(l)} < \eta_{qe}\eta_{qd}^{(f)}$ the opposite situation holds. For each laser wavelength λ_l the crossing point between these two cases corresponds to a definite value of the emission quantum efficiency $\eta_{qe}^{cross}(\lambda_l) = \overline{\lambda}/\lambda_l$, i.e. to a well defined doping concentration and is independent on the pump wavelength. For instance, in case of the Nd:YAG, the crossing points for the main laser wavelengths are $\eta_{qe}^{cross}(946\text{nm}) = 1.097$, $\eta_{qe}^{cross}(1\,064\text{nm}) = 0.976$ and $\eta_{qd}^{cross}(1\,320\text{nm}) = 0.786$. Since, by definition, $\eta_{qe} \le 1$, in case of the quasi-three laser emission at 946 nm $\eta_h^{(l)}$ is always smaller than $\eta_h^{(f)}$, whereas in case of the 1 064 nm and 1 320 nm lasers such situation is installed only above a certain Nd concentration, 0.109 at:% in the first case and 1.08 at.% in the second.

From the definition of the global heat load parameter, Eq. (13), the heat load parameter does not change suddenly from the value given by Eq. (14) below threshold to that given by Eq. (15) above threshold but follows a gradual transition described by Eq. (13) and determined by the laser emission efficiency η_l, *i.e.* by the operating point above threshold and by the superposition of the laser mode and pumped volumes η_v, to a value that could be still different from $\eta_h^{(l)}$. However, the dependence of the generated heat power on the pump power will show two segments of linear dependence that change the slope from $\eta_h^{(f)}$ to the value of $\eta_h^{(l)}$ amended for the actual value of η_v. This discussion of the heat generation is strictly valid for pure four-level laser schemes. However, in case of quasi-three-level schemes, the partial reabsorption of the laser radiation can increase the heat load coefficient. In this case the heat loading can be reduced by operating at very high pump power to saturate the reabsorption of by reducing the temperature in order to lower the thermal population of the terminal laser level.

3.4. SPATIAL DISTRIBUTION OF THE DE-EXCITATION PROCESSES

In absence of laser emission the distribution of the absorbed power determines a similar distribution of heat generation in the laser material. However, in presence of laser emission the difference in the heat generation between the ions

that participate to laser emission and those that do not lase can modify the distribution of heat generation in a way determined by the operating point above the laser threshold P/P_{th} and by the superposition of the laser mode and the pumped volume as well as by the emission quantum defect (pump wavelength) and quantum efficiency (doping concentration).

4. ENGINEERING OF LASER EMISSION AND OF HEAT GENERATION

The explicit dependence of the global efficiencies of the de-excitation processes (Eqs. (11–13)) and of the laser parameters (Eqs. (5–7)) on the individual efficiencies of the various steps in the flow of excitation inside the pumped laser material enable selection of the laser material and pumping characteristics that would enable optimization of laser emission and limitation of heat generation. A major factor that influences these processes is the laser quantum defect. The laser emission processes on different transitions assume several fixed system parameters, such as the positions of the emitting and terminal laser levels. However, as discussed above, the pump level is selected on arguments based on the availability of pumping sources and on pump absorption efficiency. This could suggest reduction of the global quantum defect by pumping directly into the emitting level, with elimination of the upper quantum defect. The emission quantum defect could be further reduced by using for pumping absorption transitions that originate from excited Stark levels of the ground state of the laser ions (hot bands): the reduced absorption because of lower thermal population of these Stark levels could be compensated in several system by the accidental degeneracy of absorption bands originating from two or more excited levels, whose summed fractional thermal population could exceed that of the ground level.

The Nd lasers are traditionally pumped by arc- or flash-lamps in various absorption lines in the visible range or by continuous-wave (CW) or quasi-continuous-wave (QCW) diode lasers in the strong absorption line in the 808 nm range between the lowest Stark levels of the ground level $^4I_{9/2}$ and of the level $^4F_{5/2}$, placed about 850–900 cm^{-1} above the emitting level $^4F_{3/2}$. The lamp pumping of the Nd lasers induces very large laser quantum defect and severe heating of the laser material and is now limited to the high-energy pulse lasers, for which suitable pump diode laser are not available. However, CW pumping of the Nd lasers is now preferentially made with the 809 nm diode lasers.

The absorption lines into the emitting level $^4F_{3/2}$ of Nd^{3+} in YAG have quite low cross-sections and the absorption coefficients at the low Nd concentrations specific to the Nd:YAG crystals (around 1 at.%) are small. However, with the advent of polycrystalline materials produced by ceramic techniques, fabrication of highly doped (to 9 at.%) Nd:YAG laser materials become possible [16, 17]. High-resolution static and dynamic spectroscopic investigation of these materials [6, 15,

18-22] indicated that the energy level structure, the transition cross-sections, the emission decay and the energy transfer parameters are similar to those of the corresponding Nd:YAG crystals. Moreover, the laser emission characteristics of the Nd:YAG ceramics proved similar to those of single crystals.

The room temperature absorption spectrum of the highly doped ceramics (Fig. 3) evidences several transitions whose absorption coefficient becomes large enough for efficient direct diode laser pumping, the most intense individual transition being that between the lowest Stark component of the ground manifold and the second Stark component of the emitting level, $^4I_{9/2}(1)\rightarrow{}^4F_{3/2}(2)$ at 869 nm: for the 1 at.% ceramic the peak absorption coefficient for this line is ~4 cm^{-1} and the line is quite narrow (below 1 nm); the intensity of this line increases slightly non-linearly with Nd concentration because of the concentration broadening of the line (about 10% in the 1-to-9 at.% Nd). Pumping into this line would increase the Stokes ratio λ_p/λ_l by ~7.4 % and reduce the relative quantum defect for the 1 064 nm laser emission by ~23.6% compared with the 809 nm pumping; however, the small linewidth compared with the usual 2-3 nm linewidth of the 809 nm diode lasers reduces the efficiency of pumping. More promising in this respect looks the two-peaked absorption band centered at 885 nm that collects the thermally-activated (hot-bands): although its absorption coefficient for 1 at.% Nd is 1.65 cm^{-1}, the larger linewidth (~3 nm) makes the diode laser pumping more efficient: Moreover, pumping at 885 nm increases the Stokes ratio by ~ 9.5 % , leading to similar improvement of the laser parameters and reduces the relative quantum defect by ~30% leading to similar reduction of heat generation compared with the traditional 809 nm pumping. This reduction can be of the order of 50% in case of the 0.9 micron emission, 30% for the one-micron lasers and 15% for the 1.3 micron lasers and manifests in higher beam quality over a higher pump power range, which could enable considerable power scaling of the Nd lasers.

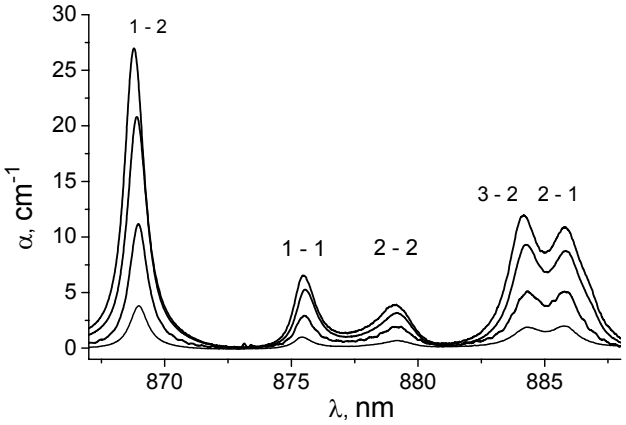

Fig. 3 – 300K absorption spectra of 1; 3.4; 6.6 and 8 at.%) Nd:YAG ceramics.

The effect of pump wavelength and of the operating point in absorbed power on the efficiencies of de-excitation processes in Nd:YAG is illustrated in case of 1 064 nm laser emission in Fig. 4, where $P = 1$ corresponds to the 809 nm pumped 1 at.% material. This figure shows that whereas the luminescence efficiency $\eta^{(l)}$ is the same regardless of pump wavelength, the laser efficiency $\eta^{(l)}$ increases at higher $\eta_{qd}^{(l)}$ on the expense of η_h. Besides the reduction of the quantum defect, the hot band pumping contributes to the stability of laser emission in a larger temperature range. Indeeed, with raising of temperature due to heat generation, the thermal population of the first Stark component of manifold $^4I_{9/2}$ decreases, that of the second component remains almost constant, whereas that of the upper components increase, with influence on the effective pump absorption component. By proper engineering of pump absorption, transitions originating from any of the Stark components of the ground manifold, even the highest ones, could be utilized for pumping, with corresponding reduction of the laser quantum defect.

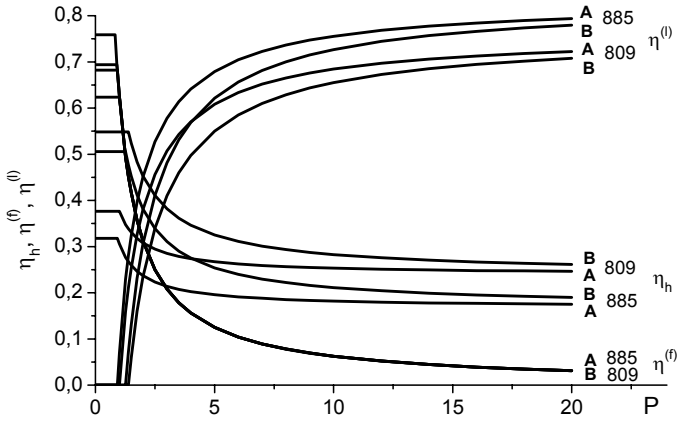

Fig. 4 – The efficiencies of de-excitation processes in Nd:YAG: A-1 at.% Nd, B-2at.% Nd.

The benefit of hot-band pumping in case of Nd lasers was demonstrated on a quite large variety of active materials, in all three main wavelength ranges. Most of these studies refer to the enhancement of laser emission parameters in the one-micron lasers of Nd-doped garnets such as YAG crystals [23-26] and ceramics [18-20], vanadates [23, 27-33], tetrafluorides [34], and so on. Beneficial effects were reported in case of the 1.3 micron lasers in case of the Nd-doped garnet [35], vanadates [36] or fluoride [37] materials. The highest enhancement of laser performances was reported, as expected, in case of the quasi-three-level Nd lasers, such as YAG [38, 39], vanadates [40], hexa-aluminates [41], fluorides [42] and so on: for some of these materials the quantum defect can be reduced to several %. In

most of these studies the enhancement of the laser parameters compared with the traditional 800 nm diode laser pumping was higher than expected from the quantum defect and this was attributed to the enhanced laser beam quality determined by the reduced thermo-optical effects. Reduction of heating under direct pumping was also demonstrated by direct measurement of the temperature in the pumped laser material [43]. Enhancement of the fundamental laser emission parameters of the Nd-doped materials under direct pumping is further accentuated (with the order of process) in the non-linear devices using this radiation [44].

In order to evidence the effect of direct pumping on the flow of excitation inside the laser material, many of these studies investigate the effect on the laser parameters expressed in absorbed pump power. However the reduced pump absorption in many laser materials at the wavelength of direct pumping can influence adversely the laser parameters expressed in incident pump power, that determine ultimately the practical performances. As mentioned above, increasing of Nd concentration enhances the efficiency of the self-quenching processes, leading to higher laser threshold and heat generation, and by this reason many authors eliminated this approach from consideration. It was however argued that a detailed account of all effects of increased Nd concentration demonstrates that the increase of laser threshold in absorbed power can be compensated in a quite large range of concentrations by the increased pump absorption; moreover, the increased absorption has net beneficial effect on the slope and optical-optical efficiencies (Eqs. (6) and (7)). It was thus inferred that a figure-of-merit (F-o-M) for the effect of Nd concentration would be the product $\eta_a \eta_{qe}$, which by practical reasons can be simplified to the approximate "material-only" F-o-M $\alpha\eta_{qe}$ [15, 18-20]. These F-o-Ms could be further enriched by multiplying with the Stokes ratio in order to evidence the effect of the pump wavelength. However, in order to account for the effect of heating and thus the capability of scaling the CW Nd lasers to higher power, a more complex generalized figure of merit $\eta_{sc} = \eta_{o-o}^{(inc)} / \eta_h$ can be introduced [45]. Figure 4 shows the dependence of such generalized F-o-M on Nd concentration, operating point and pump wavelength in case of Nd:YAG assuming lossless laser material, high superposition of laser and pump volumes (η_v=1) and size of laser material that grants complete absorption at the two pump wavelengths.

Figure 5 indicates that direct pumping at 885 nm of the Nd:YAG lasers enables much higher utilization of the pump radiation for laser emission than the traditional 809 nm pumping and can increase the power scaling ability, i.e. the laser power for similar heat generation, by a factor of up to 1.56. This approach could enable additional scaling of the existing hundred kW ceramic Nd:lasers by amounts of the order of 50 kW by replacing the actual 809 nm pumping by 885 nm pumping.

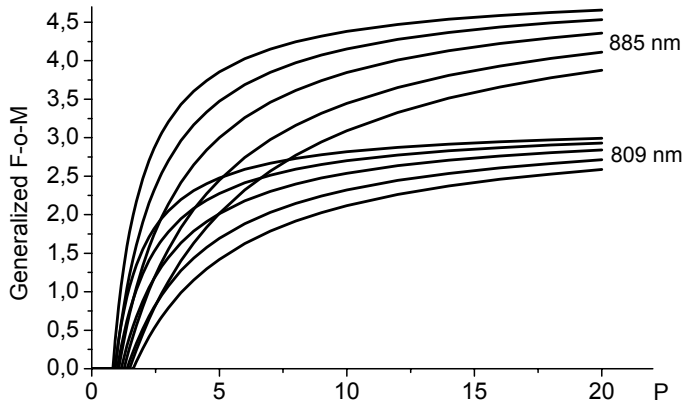

Fig. 5 – Generalized F-o-M for Nd:YAG lasers pumped at 885 nm or 809 nm. Nd concentrations in ascending order, 2.5, 2, 1.5, 1 and 0.5 at.%

Improvement of laser parameters and reduction of heat generation can be obtained by selective resonant pumping of the Yb^{3+} lasers. The Yb-doped materials give laser emission from the lowest Stark level of the unique excited manifold $^2F_{5/2}$ to the third or fourth Stark levels of the ground manifold $^2F_{7/2}$ [46]. The absorption spectra of Yb^{3+} are dominated by the very sharp (in many cases well below 1 nm) $^2F_{7/2}(1)\rightarrow{}^2F_{5/2}(1)$ line in the region 965-980 nm, that is difficult to pump by the conventional diode lasers; more suitable being the broader $^2F_{7/2}(1)\rightarrow{}^2F_{5/2}(2)$ line in region of 940 nm, which is closely accompanied by a fairly strong vibronic satellite of the first transition, whose intensity is enhanced by resonant electron-phonon interaction [47]. The 940 nm pumping of Yb laser materials determines a quantum defect of ~9.5%, much smaller than for the 1 064 nm Nd lasers, and less heat generation. However, the quite small absorption cross-section in the 940 nm region requires high doping concentrations or/and long path of pump radiation inside the laser material (such as in the multi-pass disk lasers or in the fiber lasers), which could introduce additional limiting factors [48]. Recent development of narrow-band diode lasers and of frequency stabilization techniques could determine strong impetus for pumping into the much stronger $^2F_{7/2}(1)\rightarrow{}^2F_{5/2}(1)$ absorption line moreover, although the second Stark level of the excited $^2F_{5/2}$ is close to the first (several hundred cm^{-1}), elimination of the upper quantum defect could reduce drastically the global quantum defect, in many cases well above 50%, with corresponding reduction of heat generation. Unfortunately, the extreme narrow width of this transition at the cryogenic temperatures that transforms the Yb lasers in four-level lasers [49-51] could limit this approach to the room temperature lasers. Various techniques for additional reduction of the global heat generation, such as the radiation-balanced laser emission could be beneficial for construction of very stable Yb lasers [52, 53]. Whereas transitions for hot-band pumping are not identified in the Yb laser materials, such approach can be used for the quasi-three-level Er^{3+} lasers, where such situation can be met in many materials.

5. CONCLUSION

Analysis of the de-excitation processes in a pumped laser material shows that the global efficiencies of the laser, luminescence and heat generation can be described by the various steps of excitation inside the energy level scheme of the laser ion. This analysis evidences two main sources of heat generation, the quantum defect of the radiative processes and the non-radiative de-excitation of the emitting level by energy transfer and electron-phonon interactions. Reduction of the quantum defect can be, in principle, made by pumping directly into the emitting laser level; further reduction can be made by using thermally activated absorption lines, particularly degenerated lines involving several electronic transitions. For complex laser ions, such as Nd^{3+}, the direct pumping transitions could have quite small absorption cross-sections and this determines the need for concentrated laser materials that, in turn, could enhance the self-quenching of luminescence. It is shown that the global effect of the doping concentration and of the pump wavelength can be accounted for by introducing relevant figures-of-merit and the dependence of these F-o-M on the characteristics of the laser material (doping concentration, size) and of the pumping system (wavelength, intensity) enables selection of conditions for simultaneous enhancement of laser parameters and reduction of heat generation, resulting in considerable power scaling ability.

Acknowledgements. This work was supported by CNCSIS –UEFISCSU, project number PNII – IDEI code 1240, 503/2008.

REFERENCES

1. W. Koechner, *Solid-State Laser Engineering*, 6th ed., Springer, New York, 2006.
2. W. A. Clarkson, J. Phys. D: Appl. Phys., **34**, 2381 (2001).
3. D. P. Devor, L. G. De Shazer, and R. C. Pastor, IEEE J. Quantum Electron., **25**, 1863 (1989).
4. T. Y. Fan, IEEE J. Quantum Electron., **29**, 1457 (1993).
5. V. Lupei, A. Lupei, C. Tiseanu, S. Georgescu, C. Stoicescu, P. M. Nanau, Phys. Rev. B., **53**, 8 (1995).
6. V. Lupei, Opt. Mat., **19**, 95 (2001).
7. B. R. Judd, Phys. Rev., **127**, 75 (1962).
8. G. S. Ofelt, J. Chem. Phys., **37**, 511 (1962).
9. Th. Forster, Ann. Phys. (Leipzig), **2**, 55 (1948).
10. D. L. Dexter, J. Chem. Phys., **21**, 836 (1953).
11. M. Inokuti, F. Hirayama, J. Chem. Phys., **43**, 1978 (1965).
12. I. S. Golubov, Yu. V. Konobeev, Sov. Phys. Solid State. **13**, 2679 (1972).
13.V. Lupei, A. Lupei, S. Georgescu, I. Ursu, Appl. Phys. Lett., **59**, 905 (1991)
14. V. Lupei and A. Lupei, Phys. Rev., **B61**, 8087 (2000).
15. V. Lupei, A. Lupei, S. Georgescu, T. Taira, Y. Sato, A. Ikesue, Phys. Rev. B. **64**, 092102 (2001)
16. A. Ikesue, T. Kinoshita, K. Kamata, K. Yoshida, J. Am. Ceram. Soc**., 78**, 1033 (1995).
17. J.Lu, M. Prabhu, J. Song, C. Li, J. Xu, K. Ueda, A. A. Kaminskii, H. Yagi, T. Yanagitani, Appl. Phys. B, **71**, 469 (2000).

18. V. Lupei,T. Taira, A. Lupei, N. Pavel, I. Shoji, A. Ikesue, Opt. Commun., **195**, 225 (2001).
19. V. Lupei, A. Lupei, S. Georgescu, B. Diaconescu, T. Taira, Y. Sato, S. Kurimura, A. Ikesue, J. Opt. Soc. Am. B, **19**, 360 (2002).
20. V. Lupei, A. Lupei, N. Pavel, I. Shoji, T. Taira, A. Ikesue, Appl. Phys. Lett., **79**, 590 (2001).
21. V. Lupei, A. Lupei, A. Ikesue, J. Alloys. Comp.**, 380**, 61 (2004).
22. V. Lupei, A. Lupei, A. Ikesue, Opt. Mat., **130**, 1781 (2008).
23. R. Lavi, S. Jackel, Appl. Opt., **39**, 3093 (2000).
24. V. Lupei, N. Pavel, T. Taira, Opt. Lett., **26**, 1678 (2001).
25. Z. Huang, Y. Zhang, Y. Chen, Z. Luo, J. Opt. Soc. Am. B, **22**, 2564 (2005).
26. S. Goldring, R. Lavi, Opt. Lett., **33**, 669 (2008).
27. V. Lupei, N. Pavel, T. Taira, Opt. Commun., **201**, 431 (2002).
28. V. Lupei, N. Pavel, Y. Sato, T. Taira, Opt. Lett.**, 28**, 2366 (2003).
29. L. Mc Donaugh, R. Wallenstein, R. Knappe, A. Nebel, Opt. Lett., **31**, 3297 (2006).
30. Y. F. Lu, J. Xia, X. D. Yin, D. Wang, X. H. Zhang, Laser Phys. Lett., **7**, 11 (2010).
31. Y. F. Lu, X. H. Zhang, J. Xia, Laser Phys. Lett., **7**, 487 (2010).
32. J. L. Ma, B. Xiong, L. Quo, P. F. Zhao, L. Zhang, X. C. Lin, J. M. Li, Q. D. Duanmu, Laser Phys. Lett., **7**, 579 (2010).
33. X. Delen, F. Balembois, O. Musset, P. Georges, J. Opt. Soc. Am. B, **28**, 521 (2011).
34. F. D. Zhang, X. H. Zhang, W. Liang, C. L. Li, Laser Phys., **21**, 639 (2011).
35. N. Pavel, V. Lupei, T. Taira, Opt. Express, **13**, 7948 (2005).
36. N. Pavel, T. Dascalu, N. Vasile, V. Lupei, Laser Phys. Lett., **6**, 38 (2009).
37. C. L. Li, X. H. Zhang, W. Liang, Z. M. Zhao, Laser Phys., **21**, 340 (2011).
38. V. Lupei, G. Aka, D. Vivien, Opt. Commun., **204**, 399 (2002).
39. V. Lupei, N. Pavel, T. Taira, Appl. Phys. Lett., **81**, 2677 (2002).
40. Y. F. Lu, J. Xia, X. H. Zhang, Laser Phys. Lett., **7**, 120 (2010).
41. V. Lupei, G. Aka, D. Vivien, Opt. Lett., **31**, 1064 (2006).
42. W. Liang, X. H. Zhang, Z. L. Liang, Y. Q. Liu, Z. Liang, Laser Phys., **21**, 320 (2011).
43. N. Pavel, V. Lupei, J. Saikawa, T. Taira, H. Kan, Appl. Phys. B, **82**, 599 (2006).
44. V. Lupei, N. Pavel, T. Taira, Appl. Phys. Lett., **83**, 3653 (2003).
45. V. Lupei, Opt. Mat., **31**, 701 (2008).
46. L. D. DeLoach, S. A. Payne, L. K. Smith, W. K. Kway, W. F. Krupke, J. Opt. Soc. Am. B, **11**, 269 (1994).
47. A. Lupei, V. Lupei, C. Presura, V. N. Enaki, A. Petraru, J. Phys. Condens. Mat., **11**, 3769 (1999).
49. S. Chenais, F. Druon, S. Forget, F. Balembois, P. Georges, Prog. Quantum Electron., **30**, 89 (2006).
49. D. C. Brown, IEEE J. Sel. Top. Quantum Electron., **11**, 587 (2005).
50. T. Y. Fan, D. J. Ripin, R. L. Aggarwall, J. Sel. Top. Quantum Electron, **13**, 448 (2007).
51. G. L. Bourdet, O. Casagrande, N. Deguil-Robin and B. Le Garrec, J. of Phys.: Conf. Series, **112**, 032054 (2008).
52. S. R. Bowman, IEEE J. Quantum Electron., **35**, 105 (1999).
53. G. Nemova, R. Kashyap, Rep. Prog. Phys., **73**, 086501 (2010).